Intercomparison of nanodosimetric distributions in nitrogen simulated with Geant4 and PTra track structure codes

Marcin Pietrzak, Heidi Nettelbeck, Yann Perrot, Carmen Villagrasa, Aleksandr Bancer, Marion Bug, Sebastien Incerti

Intercomparison of nanodosimetric distributions in nitrogen simulated with Geant4 and PTra track structure codes

Marcin Pietrzak[a,e,*], Heidi Nettelbeck[b,e], Yann Perrot[c,e,f], Carmen Villagrasa[c,e,f], Aleksandr Bancer[a,e], Marion Bug[b,e], Sebastien Incerti[d,f]

[a] National Centre for Nuclear Research (NCBJ), Andrzeja Sołtana 7, 05400 Otwock, Poland
[b] Physikalisch-Technische Bundesanstalt (PTB), Bundesallee 100, 38116 Braunschweig, Germany
[c] Institut de Radioprotection et de Sûreté Nucléaire (IRSN), 31 avenue de la Division Leclerc, 92260 Fontenay-Aux-Roses, France
[d] Université de Bordeaux, CNRS, LP2I Bordeaux, UMR 5797, 19 Chemin du Solarium, 33170 Gradignan, France
[e] European Radiation Dosimetry Group e.V. (Eurados), Ingolstädter Landstrasse 1, Neuherberg, 85764, Germany
[f] Geant4-DNA collaboration

Abstract

To facilitate the use of Geant4-DNA for radiation transport simulations in micro- and nanodosimeters, which are physically operated with tissue-equivalent gases such as nitrogen (and propane), this work aims to extend the cross section data available in Geant4-DNA to include those of nitrogen for electron energies ranging from 1 MeV down to the ionisation threshold. To achieve this, interaction cross section data for nitrogen that have been used with the in-house PTB PTra track structure code have been implemented in the current state-of-the-art Geant4-DNA simulation toolkit. An intercomparison has been performed between the two codes to validate this implementation. To quantify the agreement between the cross section models for nitrogen adopted in PTra and those implemented in Geant4-DNA, the simulation results of both codes were analysed using three physical parameters describing the ionisation cluster size distribution (ICSD): mean ionisation cluster size, variance of the cluster size and the probability to obtain a single ionisation within the target. Statistical analysis of the results indicate that the interaction cross section models for nitrogen used in PTra (elastic scattering, impact ionisations and electronic excitations) have been successfully implemented in Geant4-DNA. In addition, simulated ICSDs were compared to those measured with the Jet Counter nanodosimeter for energies between 100 and 2000 eV. For greater energies, the ICRP data for LET and particle range were used as a reference. The modified Geant4-DNA code and data successfully passed all these benchmarks fulfilling the requirement for their public release in the next version of the Geant4 toolkit.

Keywords: nanodosimetry, Geant4-DNA, particle track structure, ionising radiation, Monte Carlo simulation, electron cross sections

1. Introduction

Fundamental knowledge of the mechanisms driving ionising radiation interactions with biological targets is the key to answer many questions that persist in the field of radiation protection, particularly for medical applications. Being able to adapt current approaches for dosimetry to novel radiation therapy treatments, such as hadrontherapy, BNCT (boron neutron capture therapy) or the use of metal nanoparticles as radiosensitisers [1], as well as addressing questions related to exposure at very low doses (where only stochastic effects are expected), are just some of the research challenges that would benefit from such knowledge.

Whilst achieving a complete picture of how biological effects are induced by ionising radiation might be seen as a long-term goal, significant experimental and computational research conducted during the last decades have advanced our understanding of the different processes leading to radiation-induced effects. In this context, Monte Carlo (MC) track structure codes [2, 3] are a powerful means to simulate, on an event-by-event basis, the detailed pattern of radiation interactions (on the nanometer scale) with individual intracellular molecules, which are at the origin of these effects. For that purpose, track structure codes include the interaction cross sections needed to transport electrons down to energies of a few eV. While this method may be controversial for charged particles with kinetic energies lower than 1 keV [4], it has been argued [5] that statistical results obtained with MC track structure codes do provide a good approximation of multiple quantum scattering down to electron energies in the order of 10 eV.

Generally, track structure codes aim to include cross sections for calculating the probability of interactions that lead to energy deposition in condensed matter. In the case of low-energy charged particles, the interaction probability

*Corresponding author.
Email address: marcin.pietrzak@ncbj.gov.pl (Marcin Pietrzak)

not only depends on the atomic composition of the target, but also on its aggregation state (i.e. gas, liquid or solid). Hence, there is an additional complexity to obtain interaction cross sections experimentally. For liquid water, which is considered one of the most abundant components of biological materials, few experimental cross sections exist [6, 7]. Nevertheless, most track structure codes for radiobiological modelling use liquid water as a surrogate for all biological target materials, such as the cell nucleus or DNA [8, 9].

Existing experimental approaches, however, cannot provide any measurable quantities describing particle track structure on the nanometric scale in liquid water. Even the use of low-pressure water vapour in experimental setups is challenging. Thus, the most common experimental approach is to use more inert gases like nitrogen or propane. For example, microdosimeters often use tissue-equivalent gases comprising a mixture of propane, nitrogen and carbon dioxide, while nanodosimeters are usually operated with nitrogen or propane [10].

MC tools capable of simulating such experiments are not only scarce, but also challenging to develop and implement. In the case of nitrogen, one of the most tested MC track structure codes is the PTra code developed at PTB [11–13]. The code has been successfully applied to simulate experiments, in particular, those performed using three different nanodosimeters using nitrogen or propane as a target gas [12, 14–19].

Written in FORTRAN, the PTra code provides a rudimentary interface regarding the target and beam geometry. Only simple geometries can be easily implemented and anything more complicated demands careful changes in many of the subroutines, which is prone to human error. One solution is to implement appropriate cross section models for these gases in a more contemporary and open source MC toolkit such as Geant4 [20], which provides a more versatile interface for defining beam and detector geometries. Furthermore, the widespread use of Geant4 compared to the PTra code would enable the simulation tools based on such cross-section data to be available to more scientific users.

The Geant4-DNA collaboration therefore initiated a new activity to implement interaction cross section data of materials other than liquid water for track structure simulations. This began with four DNA-substitute materials tetrahydrofuran (THF), trimethyl phosphate, (TMP), purine (Pu) and pyrimidine (Py), which were already implemented in PTra [13], and has been furthered in this work with the inclusion of nitrogen. In future releases, it is planned to also include cross section data for propane. For this purpose, specific model classes were designed and implemented in the Geant4-DNA extension of the Geant4 code (i.e. in the Geant4DNAPTB model classes) [9, 21–23]. Currently, these publicly available models can be used to perform track structure simulations in the four DNA-substitute materials mentioned above, as demonstrated in the Geant4 "ICSD" user example [9, 24].

In this work, we validate the inclusion of appropriate cross section models for nitrogen in Geant4-DNA prior to its public release. Using these newly implemented data, the ability of the modified Geant4-DNA toolkit to simulate certain physical track-structure quantities is benchmarked against the PTra code in which the cross sections were first implemented. Physical track structure quantities relevant to nanodosimetry, such as the ionisation cluster size distribution (ICSD), were simulated with both Geant4-DNA and PTra using identical cross section data. In the course of comparing the transport methods and models adopted in both codes, some minor bugs were corrected in the PTra code. A validity check of the simulation results (obtained with the new cross section data) was carried out by benchmarking the simulated electronic stopping power and range in nitrogen with corresponding ICRU and NIST data [25] for energies greater than 10 keV. For energies less than 10 keV, the comparison was made against a model presented by Gümüş [26]. In this low energy range, simulated ICSDs were also compared to those obtained experimentally (in nitrogen) by Bancer (aka Bantsar) *et al.* using the Jet Counter nanodosimeter at NCBJ [27]. The good agreement between Geant4-DNA and PTra codes for simulated quantities such as ICSDs as well as experimental results and published data on stopping power and range values satisfies the requirement for their release in the Geant4 code. Furthermore, it facilitates the next stage of this work, which is the implementation in the same model classes of interaction cross section data for propane.

In a broader context, this work is aligned with the Geant4 developers' initiative to provide a well-documented and tested open source MC tool for a variety of medical physics applications, from radiation quality studies through radiobiology to patient treatment with radiotherapy [28].

2. Materials and methods

2.1. Physical processes and models for nitrogen electron interactions

With the aim of validating the implementation of nitrogen cross sections in Geant4-DNA classes, this study compares the performance of the MC track structure codes Geant4 (version 10.06.p01) and PTra (versions V10/08 and V22/04) using identical interaction cross section data for nitrogen. The key features of the cross section models are extensively described by Grosswendt and Waibel [11] with further amendments in [12, 13]. An overview of these models is given in Table 1 and a brief description is provided in the subsequent sections.

In the case of Geant4-DNA, the cross sections were implemented in the form of lookup tables so that they can be easily replaced, if needed, in a future revised version of the code. For example, it is planned to introduce an alternative elastic scattering model for nitrogen based on recent

Table 1: Summary of the models used to calculate interaction cross sections in nitrogen, which were obtained from PTra and then implemented in Geant4-DNA.

Interaction type	**Cross section type**	**Models**
Impact ionisation	**Total (including partial cross sections for subshells)**	Binary-Encounter-Bethe (BEB) model [29], except for K-shell ionisation which uses one proposed by Casnati *et al.* [30].
	Differential (production energy of secondaries)	Breit-Wigner formula [31].
	Doubly-differential (production angle for given production energy)	Berger's kinematic model with an extension for low energies [11]
Elastic scattering	**Total**	Fitted experimental data [11].
	Differential (scattering angle)	Modified Rutherford model with atomic screening corrections [11].
Electronic excitation	**Total (including 29 partial cross sections)**	Formulas and cross section parameters based on Porter *et al.* [32].

experimental data for electrons of energies ranging from 30 to 1000 eV once the experimental data is published.

In all simulations and calculations, an energy cut of 15.58 eV (i.e. the ionisation threshold of nitrogen) was used for electron transport.

While interaction cross section models presented in Table 1 are implemented in the PTra code, they are often not used directly. Rather, lookup tables are generated in the initialisation phase which are then used during the simulation of track structure. The Geant4-DNA classes were therefore designed to use pre-generated lookup tables with an identical format as those used in the internal tables of PTra. A different approach, however, was used to calculate the production energy of secondaries (in the ionisation model) and the calculation of the scattering angle (in the elastic scattering model). In both cases, PTra uses formulas that directly describe particular models, while Geant4-DNA uses pre-generated lookup tables based on these formulas. This difference in code design allows the necessary generalisation of Geant4-DNA to simulate a variety of materials using different sources of cross section data, often providing alternatives for the same material. This dissimilarity between PTra and Geant4-DNA can lead to residual differences in the simulation results obtained with these codes.

2.1.1. Impact ionisation model

The Binary-Encounter-Bethe (BEB) model [33] with the molecular orbital data from Hwang *et al.* [29] is used for describing the electron impact ionisation processes in nitrogen. The model provides partial ionisation cross sections for the four subshells with binding energies of 15.58 eV, 17.07 eV, 21.00 eV and 41.72 eV. With a binding energy of 409.5 eV, the K-shell is treated separately according to the empirical formula proposed by Casnati *et al.* [30]. The energy of a secondary electron emitted after impact ionisation is determined by the Breit-Wigner formula. [31]. For any given energy, the total ionisation cross section should be the sum of the cross sections for all five subshells. However, if the auto-ionisation process is activated, as is the default behaviour in both codes, then the total impact ionisation cross section is reduced by an amount that is then added to the total excitation cross section. This auto-ionisation process corresponds to an emission of a secondary electron after the excitation of one or more nitrogen shells. Therefore, the total emission of secondary electrons produced either by ionisation or auto-ionisation must be preserved in accordance with the total ionisation yield. Compared to when it is inactivated, activation of the auto-ionisation option can lead to small variations in energy and angular distribution of secondary electrons.

2.1.2. Excitation model

In this model, there is no scattering (change in momentum direction) of incident electrons. The treatment of electronic excitation processes is based on the formulas and cross section parameters of Porter *et al.* [32]. To obtain a better agreement with the experimental total scattering cross sections, a few corrections and extensions have been applied [12].

The auto-ionisation process is part of the excitation model in both MC codes, where a probability of 50% auto-ionisation is assumed if the excitation energy of a Rydberg state is greater than the 15.58 eV ionisation threshold for nitrogen. The secondary electrons produced by auto-ionisation are emitted isotropically and their kinetic energy is calculated from the given excitation energy minus the ionisation threshold.

2.1.3. Elastic scattering model

The treatment of elastic electron scattering is based on integrated cross sections $\sigma_{\mathrm{el}}(\mathrm{T})$ obtained by experiments

and on Rutherford's differential cross sections $(d\sigma/d\Omega)_{el}$ with respect to the solid angle, which were modified to take into account atomic screening effects [11].

2.2. Auger cascades and auto-ionisation

As mentioned above, PTra has the capability of simulating auto-ionisation following an excitation as well as Auger cascades after a K-shell ionisation of the target molecule. While it is also possible to simulate Auger cascades in Geant4-DNA, both codes have different implementations of the process, which may lead to differences in the simulated results. Since the Auger cascade process is independent of the cross section implementation to be validated in this work, the Auger cascade model was inactivated in both PTra and Geant4-DNA. The auto-ionisation process, on the other hand, was incorporated in the G4DNAPTBExcitationModel class in a similar manner to that in PTra, and thus is included in the comparison of simulated results obtained with both codes.

2.2.1. Modifications to the PTra code

Prior to implementing the physical models in Geant4-DNA, the PTra code was updated to version V22/04. This included some minor changes in an older version (V18/08) of PTra that were necessary to perform simulations for the intercomparison for specific target and beam geometries. It was during this process that a few minor bugs in PTra were identified and subsequently corrected, namely some outdated physics constants (minor differences compared to contemporary values), miscalculation of a few percent for the total ionisation cross section due to omission of the K-shell contribution in the summation (up to 100 keV of electron energy, the K-shell contribution is less than 5%), a mistake in the formula for production angles of secondary electrons with energies below 200 eV. (Owing to the limited range and high elastic-scattering cross section of these electrons, the exact angular spectrum during production is of little importance.) The overall impact of these minor bugs is only apparent during sensitive tests and, thus, in most typical cases has little effect on the simulation results. Consequently, simulated results were compared for the following versions of the codes:

1. PTra V22/04 (updated version of PTra V18/08);
2. Geant4-DNA (10.06.p01): including all cross section data derived from models implemented in PTra V22/04;
3. PTra V18/08: initial version of the PTra code used in previous studies. Simulations were performed with this version to determine the impact of the aforementioned code upgrade on the results.

2.3. Simulated geometries and energies

To compare and validate the results of both codes, different combinations of simulation geometries and energies were investigated, both with nitrogen target volumes of density equal to 1 g/cm^3 (i.e. liquid water density). The world volumes in which these targets were placed were also filled with nitrogen of density equal to 1 g/cm^3. This density was chosen to enable the simulations to be performed in target volumes of sizes equivalent to those of biological targets, such as DNA constituents. In the first geometry, a cylindrical target 2.3 nm in diameter and 3.4 nm in height (representing the typical dimensions of a DNA segment comprising 10 base pairs) was placed in the centre of a 10×10×10 nm^3 cubic world volume. The target was irradiated with a pencil beam of monoenergetic electrons originating on the side of the cylinder at half of its height. This geometry is identical to the one used in the Geant4 "ICSD" example, which is already available for simulations with DNA-substitute materials (i.e. THF, TMP, Pu and Py). The objective of this work is to extend this ICSD example (in a future Geant4 release) to include nitrogen as a potential material.

In the second geometry, a spherical target of 8 nm in diameter (representing the volume of a nucleosome) was placed at the centre of a 20×20×20 nm^3 cubic world. Both the target and world were filled with nitrogen of density equal to 1 g/cm^3. The target was irradiated by an isotropic source of monoenergetic electrons originating at the centre of the sphere. The use of these two targets allows the investigation of different ICSDs in terms of mean values and variances to cover all possible discrepancies that may arise in the results obtained with the two codes. For both geometrical setups, at least 10^7 primary electrons were simulated for each initial kinetic energy: 20 eV, 30 eV, 50 eV, 70 eV, 100 eV, 150 eV, 200 eV, 300 eV, 400 eV, 500 eV, 600 eV, 800 eV, 1 keV, 2 keV, 3 keV, 5 keV, 10 keV, 20 keV, 50 keV, 100 keV, 200 keV, 500 keV and 1 MeV, which led to results with statistical uncertainties of less than 1%.

2.4. Comparison with experimental data

Simulated ICSDs were also compared with those obtained experimentally in order to benchmark the cross section data implemented in both Geant4-DNA and PTra codes. Measured ICSDs for low-energy monoenergetic electron beams traversing a "nanometric" nitrogen target are reported by Bancer *et al.* [27, 34]. The study includes a detailed description of the Jet Counter nanodosimeter and experimental setup used to carry out the measurements.

The most important aspects of the experimental setup can be summarised as follows. The target in the Jet Counter is created dynamically by a pulse-operated piezoelectric valve that injects a jet of nitrogen gas to a interaction chamber (IC). The IC volume is an open (bottomless) cylinder, 10 mm in diameter and 10 mm in height. Following passage of the projectile, ions created within the IC escape with the gas jet to a much larger vacuum chamber. While neutral molecules dissipates within the chamber, an electric field guides all ions to a single ion detector which then counts them one-by-one. Thus, the entire IC region is a sensitive volume of the detector, in which all ions created inside are measured with a known detection efficiency.

For each event, the target was irradiated with a single pulse from the electron gun. The average number of electrons per beam pulse was approximately one, but varied slightly from experiment to experiment (see Table 2). Despite the real number of electrons for any given event being random, it was verified to obey a Poisson process. This of course means that some events were blank shots (no electron was emitted from the electron gun). In order to compare these measurements with simulations, a Poisson probability distribution for the number of electrons per each event was taken into account.

The nitrogen gas density within the nanodosimeter was tuned to a value of 0.34 µg/cm^3. Applying the scaling procedure described by Grosswendt [35], this cylindrical nitrogen volume could be scaled to a cylindrical water target of unit density (roughly 2.3 nm in both diameter and height), which is equivalent in size to a short segment of DNA. In both PTra and Geant4-DNA simulations, however, the target's geometry and density were the same as those used in the experiment.

2.5. Reference quantities

For comparison purposes, ICSD was chosen as the basic physical reference quantity as it is usually regarded as one of the fundamental descriptors of the particle track structure. It is for this reason that many papers in the field of nanodosimetry are focused on this quantity and/or its derivatives. Sensitive to different aspects of the ICSD shape, the following three parameters of the ICSD were therefore chosen for direct comparison: the mean ionisation cluster size M_1 (i.e. first moment of the ICSD), which reflects the total ionisation yield; the variance σ^2 of the cluster size, which is most sensitive to the distribution's tail; and the probability P_1 to obtain a cluster size of one (i.e. only a single ionisation in the target), which for the geometries of interest was sensitive to both the production and behaviour of secondary electrons. The latter can lead to additional ionisations, thereby significantly lowering P_1. Of these nanodosimetric quantities, M_1 is of most interest as the other two are sensitive to subtle differences in the shape of the ICSD.

The statistical uncertainty is always given as a standard deviation of a quantity. For M_1 and σ^2, the uncertainty was calculated from the statistical properties of ICSD from which the quantity is derived. For P_k (and P_1 in particular), the standard deviation is the square root of the number of counts of a given cluster size divided by the total number of events.

3. Results and discussion

Figures 1 and 2 show the energy dependence of each of the three above-mentioned quantities for PTra V22/04 and Geant4-DNA. These results should reflect the accuracy and suitability of the implemented physical models in both codes. For both of the investigated geometries,

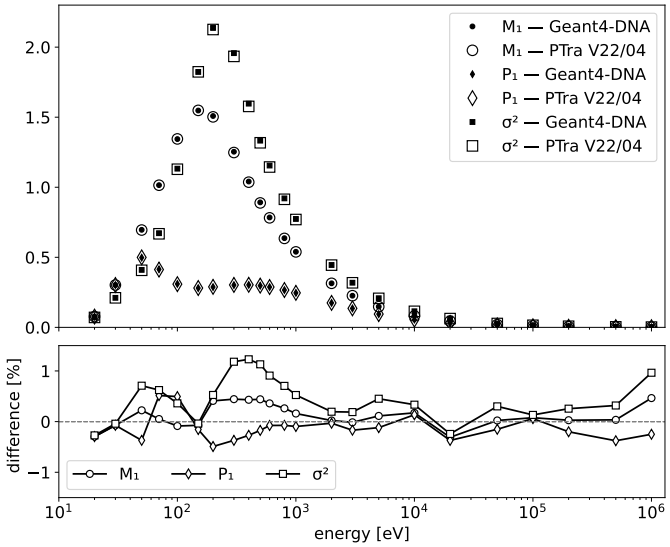

Figure 1: Energy dependence of the three quantities M_1, P_1 and σ^2 obtained with the cylindrical geometry for equivalent simulations performed using Geant4-DNA and PTra codes. The relative difference is shown in the bottom panel of the figure. Statistical uncertainties are smaller than the symbol size in both panels.

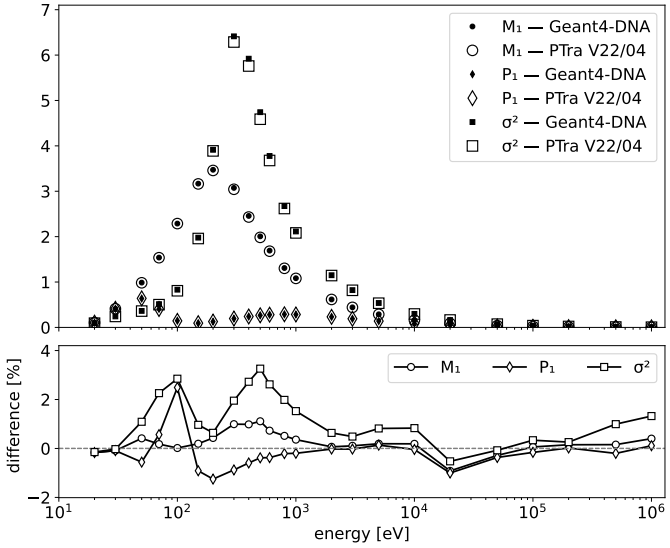

Figure 2: Energy dependence of three quantities M_1, P_1 and σ^2 obtained with the spherical geometry for equivalent simulations performed using Geant4-DNA and PTra codes. The relative difference is shown in the bottom panel of the figure. Statistical uncertainties are smaller than the symbol size in both panels.

there is a good agreement between the simulated results for all three quantities (less than ∼1% and ∼3% difference for the first and second geometries, respectively). This not only verifies the correct implementation of nitrogen cross sections in Geant4-DNA, but also suggests that the transport in both track structure codes is equivalent. Any residual (minor) discrepancies can be attributed to differences in the interpolation method of cross section values used in each respective MC code.

In the current study, the cross section models obtained

from PTra and implemented in Geant4-DNA were also validated by calculating the stopping power and range of electrons in nitrogen using equivalent implementation in both codes (i.e. PTra V22/04 and Geant4-DNA). The results of this comparison are shown in Figure 3 and 4, together with data from the NIST ESTAR database [25] (based on ICRU report 37 [36]) and Gümüş model [26]. The overestimation of the stopping power and corresponding underestimation of range is most likely related to the overestimation of impact ionisation cross sections in the BEB model (in relation to the values recommended by Itikawa [37], which was discussed by Bug *et al.* [13]). The substantial underestimation of stopping power beyond 200 keV has little impact

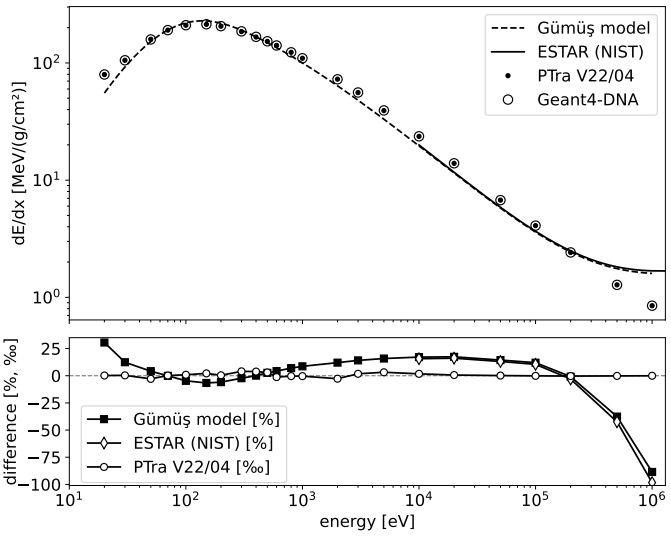

Figure 3: Energy dependence of the electronic stopping power in nitrogen for equivalent simulations performed using Geant4-DNA and PTra codes compared with data from NIST ESTAR database [25] and Gümüş model [26]. The relative difference between Geant4-DNA simulation results and the other data is shown in the bottom panel of the figure. Statistical uncertainties are smaller than the symbol size in both panels.

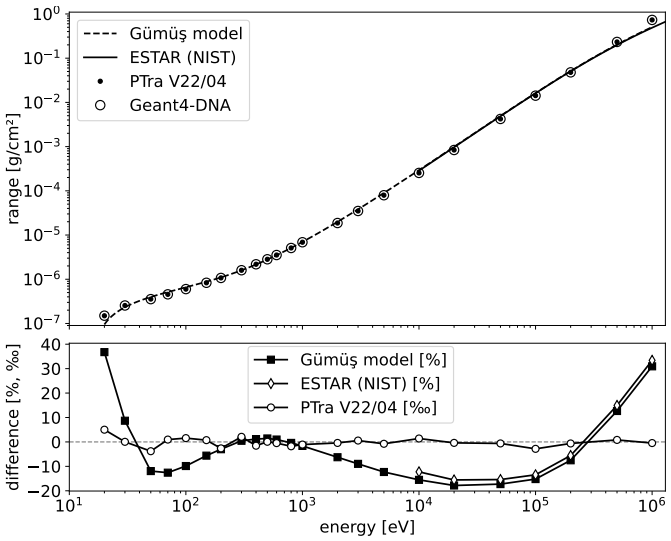

Figure 4: Energy dependence of the electron range in nitrogen for equivalent simulations with Geant4-DNA and PTra codes compared with data from NIST ESTAR database [25] and Gümüş model [26] calculated using CSDA. The cutoff energy (i.e. when electron transport is ceased) in both simulations and calculations was assumed to be 15.58 eV (nitrogen ionisation threshold). The relative difference between Geant4-DNA simulation results and the other data is shown in the bottom panel of the figure. Statistical uncertainties are smaller than the symbol size in both panels.

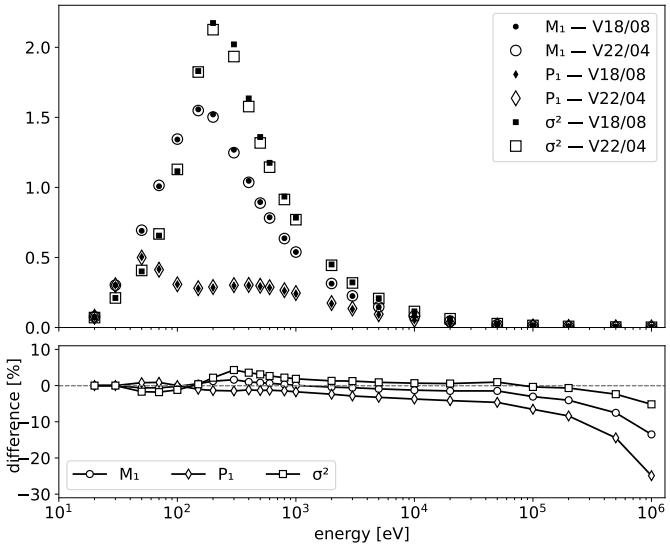

Figure 5: Energy dependence of three quantities M_1, P_1 and σ^2 obtained in a cylindrical geometry from simulations with PTra with and without updates to the code ((version V22/04 and V18/08 respectively). The relative difference is shown in the bottom panel of the figure. Statistical uncertainties are smaller than the symbol size in both panels.

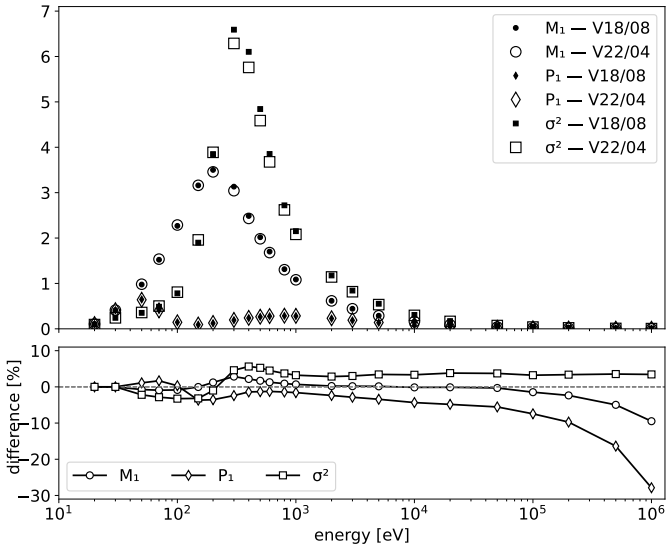

Figure 6: Energy dependence of three quantities M_1, P_1 and σ^2 obtained in a spherical geometry from simulations with PTra with and without updates to the code ((version V22/04 and V18/08 respectively). The relative difference is shown in the bottom panel of the figure. Statistical uncertainties are smaller than the symbol size in both panels.

in most applications involving radiobiology or nano- and microdosimetry. For example, in the case of a 230 MeV proton beam, which is typically the maximum initial energy of clinical beams, less than 1% of secondary electrons are produced with energies greater than 100 keV with an average value of just a few keV.

Finally, to serve as a reference for previous studies performed with earlier versions of the PTra code, we show the influence of the modifications made to PTra in this work. The overall impact of all bug fixes is shown in Figures 5 and 6, where the most significant differences are present for high-energy electrons. This suggests that the bugs present in older versions of the PTra code have little impact on any previous results for heavy charged particles (protons and alpha particles) since the upper energy limit of secondary electrons produced by primary particles in these studies was typically less than 10 keV.

3.1. Experimental validation

Figure 7 shows a comparison of the measured [27] and simulated ICSDs in nitrogen. In the interest of readability, only the simulation results obtained with Geant4-DNA are shown. (All data points obtained with both PTra and Geant4-DNA codes were found to overlap.) For the same reason, only four energies are shown. Table 2 compares the values of M_1, P_1 and σ^2 for all available experimental data.In the presented simulation results, the ionisation yield for 1 and 2 keV electron beams may be underestimated due to the absence of Auger electron cascade contributions. However, based on calculations with PTra, the impact on M_1 is in the order of 1% .

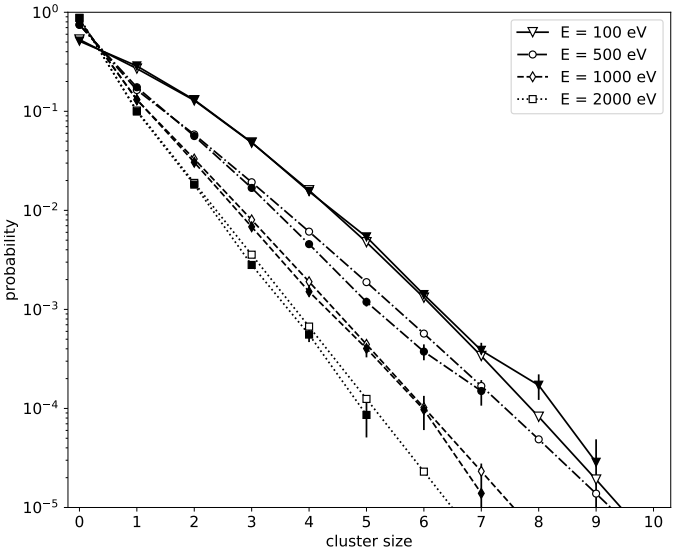

Figure 7: Comparison of the simulated (empty symbols) and measured (full symbols) ionisation cluster size distributions for different monoenergetic electron beams. The simulated cylindrical target geometry and density were identical to those adopted in the experiment (i.e. diameter and height of approximately 2.3 nm and density of 0.34 µg/cm^3. Statistical uncertainty is marked only for experimental values as for simulated it is smaller then the symbol size.

Table 2: Experimental (exp.) [27] and simulation (sim.) results for the ICSD parameters M_1, P_1 and σ^2 obtained from monoenergetic electrons of energy E traversing a nitrogen target of 0.34 µg/cm^2 thickness (i.e. equivalent geometry to that of the Jet Counter nanodosimeter). The beam intensity I is defined as the average number of primary electrons per event. Statistical uncertainties of the last digits are given in parentheses.

E [eV]	I	type	M_1	P_1	σ^2
100	1.75	exp.	0.796(4)	0.2870(21)	1.080(10)
		sim.	0.7713(4)	0.27002(17)	1.0704(8)
200	1.19	exp.	0.708(4)	0.2444(18)	1.088(10)
		sim.	0.7425(4)	0.20914(15)	1.3033(11)
300	1.02	exp.	0.542(4)	0.2133(18)	0.846(9)
		sim.	0.5685(3)	0.18649(14)	1.0122(10)
500	0.93	exp.	0.366(3)	0.1750(15)	0.541(6)
		sim.	0.3774(3)	0.16395(14)	0.6064(7)
1000	0.93	exp.	0.2221(21)	0.1317(14)	0.305(5)
		sim.	0.23101(18)	0.13029(12)	0.3279(4)
2000	1.06	exp.	0.1470(17)	0.0995(12)	0.187(3)
		sim.	0.15387(15)	0.10181(11)	0.2009(3)

4. Conclusion and further work

The results in this work indicate a successful implementation of interaction cross section models for nitrogen, namely elastic scattering, impact ionizations and electronic excitations, in the Geant4 toolkit. These cross sections are identical to those originally implemented in the PTra code, which has been used extensively over the last few decades to simulate nanodosimetric experiments. This was shown in the comparison of three physical quantities (M_1, P_1 and σ^2) describing the ICSD. A comparison of the energy dependence of these quantities with two different target geometries using Geant4-DNA and PTra V22/04 (in Figures 1 and 2) showed a good agreement between the codes. It can therefore be assumed that the transport in both MC track structure codes is similar, thus verifying a correct implementation of these cross section models for nitrogen in Geant4-DNA. Furthermore, the good agreement between the simulated stopping powers and ranges as well as ICSDs for monoenergetic electrons over the entire energy range also validates the use of these models in both codes.

Hence, these nitrogen cross sections will be included in the next release of the Geant4 code for public use. Further work is planned to extend this data set to include the implementation of appropriate cross section models for propane, which is another tissue-equivalent gas often chosen as the operating gas in micro- and nanodosimeters. This inclusion of nitrogen and propane cross section data in Geant4-DNA would not only improve the accuracy of radiation transport simulations in these media, but also increase the code's versatility for applications particularly within the micro- and nanodosimetry community.

Acknowledgements

The resources of the Świerk Computing Centre (CIŚ) financed by the EU and the Polish Ministry of Science and Higher Education (project No. POIG.02.03.00-00-013/09) were used to carry out this work.

References

[1] H. Rabus, W. Li, C. Villagrasa, J. Schuemann, P. Hepperle, L. de la Fuente Rosales, et al., Intercomparison of Monte Carlo calculated dose enhancement ratios for gold nanoparticles irradiated by X-rays: Assessing the uncertainty and correct methodology for extended beams, Phys. Medica 84 (2021) 241–253. doi:10.1016/j.ejmp.2021.03.005.

[2] H. Nikjoo, S. Uehara, D. Emfietzoglou, and F. A. Cucinotta, Track-structure codes in radiation research, Radiat. Meas. 41 (9-10) (2006) 1052–1074. doi:10.1016/j.radmeas.2006.02.001.

[3] N. Tang, Evaluation, from nanodosimetric modeling, of the influence of chromatin compaction on early radiation-induced effects and extension to late effects (DNA damage repair and cell death), Ph.D. thesis, Centre d'Etudes Nucléaires de Bordeaux Gradignan, France (Oct. 2019).
URL https://tel.archives-ouvertes.fr/tel-02399525

[4] R. M. Thomson and I. Kawrakow, On the Monte Carlo simulation of electron transport in the sub-1 keV energy range., Med. Phys. 38 (8) (2011) 4531–4534. doi:10.1118/1.3608904.

[5] D. Liljequist and H. Nikjoo, On the validity of trajectory methods for calculating the transport of very low energy (< 1 keV) electrons in liquids and amorphous media, Radiat. Phys. Chem. 99 (2014) 45–52. doi:10.1016/j.radphyschem.2014.02.015.

[6] J. M. Heller, R. N. Hamm, R. D. Birkhoff, and L. R. Painter, Collective oscillation in liquid water, J. Chem. Phys. 60 (9) (1974) 3483–3486. doi:10.1063/1.1681563.

[7] H. Hayashi, N. Watanabe, Y. Udagawa, and C.-C. Kao, The complete optical spectrum of liquid water measured by inelastic x-ray scattering, P. Natl. Acad. Sci. USA 97 (12) (2000) 6264. doi:10.1073/pnas.110572097.

[8] D. Emfietzoglou and H. Nikjoo, Accurate electron inelastic cross sections and stopping powers for liquid water over the 0.1-10 keV range based on an improved dielectric description of the Bethe surface., Radiat. Res. 167 (1) (2007) 110–120. doi:10.1667/RR0551.1.

[9] S. Incerti, A. Ivanchenko, M. Karamitros, A. Mantero, P. Moretto, H. Tran, et al., Comparison of GEANT4 very low energy cross section models with experimental data in water, Med. Phys. 37 (9) (2010) 4692–4708. doi:10.1118/1.3476457.

[10] A. Bantsar, P. Colautti, V. Conte, G. Hilgers, M. Pietrzak, S. Pszona, et al., State of the art of instrumentation in experimental nanodosimetry, Radiat. Prot. Dosim. 180 (1-4) (2018) 177–181. doi:10.1093/RPD/NCX263.

[11] B. Grosswendt and E. Waibel, Transport of low energy electrons in nitrogen and air, Nucl. Instrum. Methods 155 (1-2) (1978) 145–156. doi:10.1016/0029-554X(78)90198-2.

[12] B. Grosswendt and S. Pszona, The track structure of α-particles from the point of view of ionization-cluster formation in "nanometric" volumes of nitrogen, Radiat. Environ. Bioph. 41 (2) (2002) 91–102. doi:10.1007/s00411-002-0144-9.

[13] M. Bug, E. Gargioni, H. Nettelbeck, W. Baek, G. Hilgers, A. Rosenfeld, and H. Rabus, Ionization cross section data of nitrogen, methane, and propane for light ions and electrons and their suitability for use in track structure simulations, Phys. Rev. E 88 (4). doi:10.1103/PhysRevE.88.043308.

[14] B. Grosswendt, L. De Nardo, P. Colautti, S. Pszona, V. Conte, and G. Tornielli, Experimental equivalent cluster-size distributions in nanometric volumes of liquid water, Radiat. Prot. Dosim. 110 (1-4) (2004) 851–857. doi:10.1093/rpd/nch203.

[15] V. Bashkirov, R. Schulte, A. Breskin, R. Chechik, S. Schemelinin, G. Garty, et al., Ion-counting nanodosemeter with particle tracking capabilities, Radiat. Prot. Dosim. 122 (1-4) (2006) 415–419. doi:10.1093/rpd/ncl470.

[16] M. Bug, E. Gargioni, W. Baek, G. Hilgers, H. Nettelbeck, A. Rosenfeld, and H. Rabus, Proton-impact ionisation cross sections for nanodosimetric track structure simulations, Radiat. Prot. Dosim. 161 (1-4) (2014) 474–477. doi:10.1093/rpd/nct317.

[17] M. Bug, G. Hilgers, W. Baek, and H. Rabus, Nanodosimetric characterization of ion beams, Eur. Phys. J. D 68 (8). doi:10.1140/epjd/e2014-50015-9.

[18] G. Hilgers, M. Bug, E. Gargioni, and H. Rabus, Comparison of measuredand monte carlo simulated track structure parameters in nanometric volumes, Radiat. Prot. Dosim. 161 (1-4) (2014) 441–444. doi:10.1093/rpd/nct265.

[19] V. Conte, D. Moro, P. Colautti, and B. Grosswendt, Nanodosimetric track structure in homogeneous extended beams, Radiat. Prot. Dosim. 166 (1-4) (2015) 219–222. doi:10.1093/rpd/ncv141.

[20] S. Agostinelli, J. Allison, K. Amako, J. Apostolakis, H. Araujo, P. Arce, et al., Geant4 - a simulation toolkit, Nucl. Instrum. Meth. Adoi:10.1016/S0168-9002(03)01368-8.

[21] M. Bernal, M. Bordage, J. Brown, M. Davídková, E. Delage, Z. El Bitar, et al., Track structure modeling in liquid water: A review of the Geant4-DNA very low energy extension of the Geant4 Monte Carlo simulation toolkit, Phys. Medica 31 (8) (2015) 861–874. doi:10.1016/j.ejmp.2015.10.087.

[22] S. Incerti, G. Baldacchino, M. Bernal, R. Capra, C. Champion, Z. Francis, et al., The Geant4-DNA project, Int. J. Model. Simul. Sci. Comput. 1 (2) (2010) 157–178. doi:10.1142/S1793962310000122.

[23] S. Incerti, I. Kyriakou, M. Bernal, M. Bordage, Z. Francis, S. Guatelli, et al., Geant4-DNA example applications for track structure simulations in liquid water: A report from the Geant4-DNA Project, Med. Phys. 45 (8) (2018) e722–e739. doi:10.1002/mp.13048.

[24] M. Bug, W. Yong Baek, H. Rabus, C. Villagrasa, S. Meylan, and A. Rosenfeld, An electron-impact cross section data set (10 eV–1 keV) of DNA constituents based on consistent experimental data: A requisite for Monte Carlo simulations, Radiat. Phys. Chem. 130 (2017) 459–479. doi:10.1016/j.radphyschem.2016.09.027.

[25] NIST, ESTAR database.
URL https://physics.nist.gov/PhysRefData/Star/Text/ESTAR.html

[26] H. Gümüş, Simple stopping power formula for low and intermediate energy electrons, Radiat. Phys. Chem. 72 (1) (2005) 7–12. doi:10.1016/j.radphyschem.2004.03.006.

[27] A. Bantsar, B. Grosswendt, S. Pszona, and J. Kula, Single track nanodosimetry of low energy electrons, Nucl. Instrum. Meth. A 599 (2-3) (2009) 270–274. doi:10.1016/j.nima.2008.11.021.

[28] S. Incerti, J. M. Brown, and S. Guatelli, Advances in Geant4 applications in medicine, Phys. Medica 70 (2020) 224–227. doi:10.1016/j.ejmp.2020.01.019.

[29] W. Hwang, Y. Kim, and M. E. Rudd, New model for electron-impact ionization cross sections of molecules, J. Chem. Phys. 104 (8) (1996) 2956–2966. doi:10.1063/1.471116.

[30] E. Casnati, A. Tartari, and C. Baraldi, An empirical approach to K-shell ionisation cross section by electrons, J. Phys. B 16 (3) (1983) 505–505. doi:10.1088/0022-3700/16/3/525.

[31] A. Green and T. Sawada, Ionization cross sections and secondary electron distributions, J. Atmos. Terr. Phys. 34 (10) (1972) 1719–1728. doi:10.1016/0021-9169(72)90031-1.

[32] H. Porter, C. Jackman, and A. Green, Efficiencies for production of atomic nitrogen and oxygen by relativistic proton impact in air, J. Chem. Phys. 65 (1) (1976) 154–167. doi:doi.org/10.1063/1.432812.

[33] Y.-K. Kim and M. E. Rudd, Binary-encounter-dipole model for electron-impact ionization, Phys. Rev. A 50 (5) (1994) 3954–3967. doi:10.1103/PhysRevA.50.3954.

[34] A. Bantsar, Ionization Cluster Size Distributions Created by Low Energy Electrons and Alpha Particles in Nanometric Track

Segment in Gases, PhD Thesis, The Andrzej Sołtan Institute for Nuclear Studies (2010). arXiv:1207.6893v1.

[35] B. Grosswendt, Recent advances of nanodosimetry, Radiat. Prot. Dosim. 110 (1-4) (2004) 789–799. doi:10.1093/rpd/nch171.

[36] ICRU, Report 37. Stopping Powers for Electrons and Positrons, J. Int. Comm. Radiat. Units Meas. os-19 (2). doi:10.1093/jicru/os19.2.Report37.

[37] Y. Itikawa, Cross Sections for Electron Collisions with Nitrogen Molecules, J. Phys. Chem. Ref. Data 35 (1) (2006) 31–53. doi:10.1063/1.1937426.